

# Experimental sub-Rayleigh resolution by an unseeded high-gain optical parametric amplifier for quantum lithography.

Fabio Sciarrino<sup>2,1</sup>, Chiara Vitelli<sup>1</sup>, Francesco De Martini<sup>1</sup>, Ryan Glasser<sup>3</sup>, Hugo Cable<sup>3</sup>, and Jonathan P. Dowling<sup>3</sup>

<sup>1</sup>Dipartimento di Fisica dell'Università "La Sapienza" and Consorzio Nazionale

Interuniversitario per le Scienze Fisiche della Materia, Roma 00185, Italy

<sup>2</sup>Centro di Studi e Ricerche "Enrico Fermi", Via Panisperna 89/A, Compendio del Viminale, Roma 00184, Italy

<sup>3</sup>Hearne Institute for Theoretical Physics, Louisiana State University, Baton Rouge, LA70803

Quantum lithography proposes to adopt entangled quantum states in order to increase resolution in interferometry. In the present paper we experimentally demonstrate that the output of a high-gain optical parametric amplifier can be intense yet exhibits quantum features, namely, sub-Rayleigh fringes, as proposed by Agarwal et al. (Phys. Rev. Lett. **86**, 1389 (2001)). We investigate multiphoton states generated by a high-gain optical parametric amplifier operating with a quantum vacuum input for a gain values up to 2.5. The visibility has then been increased by means of three-photon absorption. The present article opens interesting perspectives for the implementation of such an advanced interferometrical setup.

PACS: 03.67.-a, 03.67.Hk, 42.65.Lm

## INTRODUCTION

Since the early days of Quantum Electronics, nonlinear optics has played a basic role both for its relevance as a fundamental chapter of modern science and for its technological applications [1]. Nonlinear parametric processes, due to the peculiar correlation properties of the generated photons, have been adopted to investigate the quantum properties of electromagnetic fields. In the last few years it has been proposed to exploit entangled quantum states in order to increase the resolution in quantum interferometry, specifically, for quantum lithography [2] and to achieve Heisenberg limited resolution [3]. In such framework, particular attention has been devoted to the generation of NOON states, path entangled states of the form  $\frac{1}{\sqrt{2}}(|N\rangle_{k_1}|0\rangle_{k_2} + |0\rangle_{k_1}|N\rangle_{k_2})$ , of fundamental relevance since a single-photon phase shift  $\varphi$  induces a relative shift between the two components equal to  $N\varphi$ . This feature can be exploited to enhance phase resolution in interferometric measurements, leading to a sub-Rayleigh resolution scaling as  $\frac{\lambda}{2N}$ ;  $\lambda$  being the wavelength of the field [4]. The generation of photonic NOON states has been the subject of intense theoretical research [5], but up to now the actual experimental implementation has been limited to a posteriori generation of two, three and four photons states [6, 7, 8] and to the conditional generation of a NOON state with  $N = 2$  [9]. The weak value of the generated number of photons strongly limits the potential applications to quantum lithography and quantum metrology. As alternative approach to emulate the quantum resolution, it has been proposed to adopt classical, coherent light [10] effectively exploiting the non-linearity of the absorbing material. First experimental results have been recently reported: Yablonovitch et al. proposed to use an interference technique with multiple-frequency beams achieving an experimental visibility of 3% [11] while Boyd et al. achieved a two-fold enhance-

ment of the resolution over the standard Rayleigh limit adopting a UV lithographic material excited by multiphoton absorption [12].

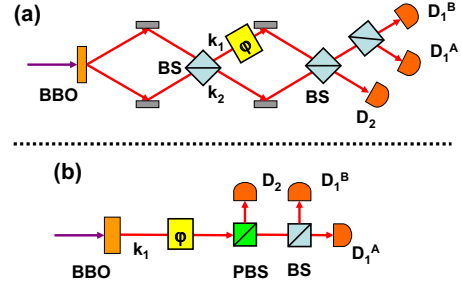


FIG. 1: (a) Experimental scheme for quantum lithography based on spontaneous parametric down-conversion. The 2-photon absorption is simulated through a 2-photon coincidence detection. (b) Configuration based on polarization entangled beams.

Recently it has been proposed to exploit a high gain optical parametric amplifier acting on the vacuum field to generate fields with a high number of photons still exhibiting sub-Rayleigh periods: Fig.1-a [13]. The quantum lithography architecture involves the generation of correlated beams over the modes  $k_1$  and  $k_2$ , the mixing over a beamsplitter (BS), the phase shifting of one mode and then the recombination of the two modes over a second BS. Finally the output state is detected via a two-photon absorption over the outgoing modes. In the typical low-gain regime the quantum state  $2^{-1/2}(|2\rangle_{k_1}|0\rangle_{k_2} - |0\rangle_{k_1}|2\rangle_{k_2})$  is generated by spontaneous parametric down-conversion (SPDC) and a Hong-Ou-Mandel interferometer adopting a post-selection technique [6]. In Ref. [13, 14, 15] it has recently been theoretically shown that, for any gain of the parametric amplifier, the two-photon excitation rate presents

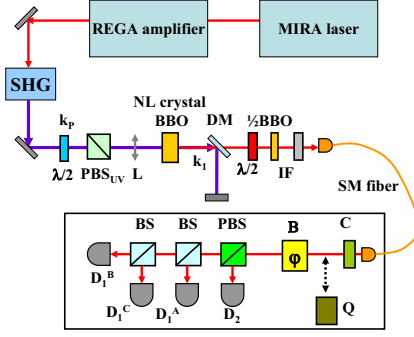


FIG. 2: Experimental layout. The radiation generated in the NL crystal is spectrally filtered by an interferential filter (IF) with bandwidth equal to 3nm and spatially selected adopting a single mode (SM) fiber.

a fringe pattern of the form  $1 + \cos 2\varphi$  which never falls below a visibility of 20%. Such an approach could lead to high resolution with a high number of photons overcoming the difficulty connected with the adoption of NOON state with a low number of photons. At variance with the scheme based on classical radiation, the one here demonstrated exploits quantum features of the OPA field.

### SUB-RAYLEIGH RESOLUTION BY AN UNSEEDED HIGH-GAIN OPTICAL PARAMETRIC AMPLIFIER

In the present paper we experimentally investigate the properties of the optical parametric amplifier (OPA) operating in the high gain regime. Instead of dealing with path entangled states, we consider the generation of entangled states over the same mode but with orthogonal polarizations, respectively, horizontal ( $\vec{\pi}_H$ ) and vertical ( $\vec{\pi}_V$ ). The scheme is shown in Fig.1-b. The non-linear crystal (BBO) is pumped by a high-power laser. The first order contribution to the output field is the twin photons state over the same mode:  $2^{-1/2}(|2\rangle_+|0\rangle_- + |0\rangle_+|2\rangle_-) = |1\rangle_H|1\rangle_V$ , with  $\vec{\pi}_\pm = 2^{-1/2}(\vec{\pi}_H \pm \vec{\pi}_V)$ . Such polarization-entangled photons can be easily converted to path entangled via an additional polarizing BS. The PBS of Fig1.b mixes the two polarization components  $\vec{\pi}_+$  and  $\vec{\pi}_-$  as the second BS of Fig1.a mixes the two different path modes, similar arrangements of polarization NOON were adopted in Ref.[7, 8].

Let us introduce the generic quantum states generated by the OPA acting on the vacuum fields  $|0\rangle_H|0\rangle_V$ . The interaction Hamiltonian of the optical parametric amplification  $\hat{H}_{coll} = i\chi\hbar\hat{a}_H^\dagger\hat{a}_V^\dagger + h.c.$  acts on the single spatial mode  $\mathbf{k}_1$ . A fundamental physical property of  $\hat{H}_{coll}$  consists of its expression for any polarization basis belonging to the equatorial basis. Indeed  $\hat{H}_{coll}$  can be written as

$\frac{1}{2}i\chi\hbar(\hat{a}_+^{\dagger 2} + \hat{a}_-^{\dagger 2}) + h.c.$  where  $\hat{a}_\pm^\dagger$  are the creation operators for the  $\vec{\pi}_\pm$  polarization modes, respectively. The output state over the mode  $\mathbf{k}_1$  of the unseeded optical parametric amplifier is found to be:

$$|\Phi\rangle = \frac{1}{C} \sum_{n=0}^{+\infty} \Gamma^n |n\rangle_H |n\rangle_V = \frac{1}{C} \sum_{i,j=0}^{+\infty} \Gamma^{i+j} |2i\rangle_+ |2j\rangle_- \quad (1)$$

with  $C \equiv \cosh g$ ,  $\Gamma \equiv \tanh g$ , being  $g$  the non linear (NL) gain [1]. This state is usually called a two-mode squeezed state. The average photon number created per polarization mode is equal to  $\bar{n} = \sinh^2 g$ . In the interferometric setup the output state is shifted by a phase  $\varphi$  in the basis  $\{\vec{\pi}_+, \vec{\pi}_-\}$ . Hence the output state is detected in the basis  $\{\vec{\pi}_H, \vec{\pi}_V\}$ ; adopting a polarizing beam splitter (PBS). For different values of the phase  $\varphi$ , the quantum state  $|\Phi\rangle$  is analyzed through two different second-order correlation functions  $G_{12}^{(2)} = \langle \Phi | c_1^\dagger c_2^\dagger c_2 c_1 | \Phi \rangle$  and  $G_{11}^{(2)} = \langle \Phi | c_1^\dagger c_1^\dagger c_1 c_1 | \Phi \rangle$  where  $\{c_1^\dagger = (\cos \frac{\varphi}{2} \hat{a}_H^\dagger - i \sin \frac{\varphi}{2} \hat{a}_V^\dagger) e^{i\frac{\varphi}{2}}, c_2^\dagger = (-i \sin \frac{\varphi}{2} \hat{a}_H^\dagger + \cos \frac{\varphi}{2} \hat{a}_V^\dagger) e^{i\frac{\varphi}{2}}\}$  are the output modes of the PBS. By tuning  $\varphi$  it is found  $G_{12}^{(2)}(\varphi) = \bar{n}^2 + \frac{1}{2}(\bar{n}^2 + \bar{n})(1 + \cos 2\varphi)$  and  $G_{11}^{(2)}(\varphi) = 2\bar{n}^2 + \frac{1}{2}(\bar{n}^2 + \bar{n})(1 - \cos 2\varphi)$  [14]. The corresponding visibilities of the obtained fringe patterns read  $V_1^{(2)} = \frac{\bar{n}+1}{5\bar{n}+1}$  and  $V_{12}^{(2)} = \frac{\bar{n}+1}{3\bar{n}+1}$ . We observe that a non-vanishing visibility is found for any value of  $g$ :  $V_1^{(2)}(g \rightarrow \infty) = \frac{1}{5}$  and  $V_{12}^{(2)}(g \rightarrow \infty) = \frac{1}{3}$ . The two fringe patterns exhibit a dependence on  $2\varphi$  and hence a period equal to  $\frac{\lambda}{2}$ . This feature can be exploited to carry out interferometry with sub-Rayleigh resolution, i.e., with fringe period lower than  $\lambda$ , in a higher flux regime compared to the two photon configurations.

### EXPERIMENTAL SETUP AND RESULTS

We now briefly describe the experimental configuration: Fig.2. The excitation source was a Ti:Sa Coherent MIRA mode-locked laser further amplified by a Ti:Sa

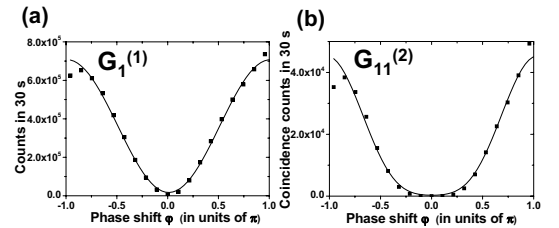


FIG. 3: Coherent state as input field. (a)  $G_1^{(1)}$ : Count rates  $D_1^A$  versus the phase  $\varphi$ . (b)  $G_{11}^{(2)}$ : Coincidence counts  $[D_1^A, D_1^B]$  versus the phase  $\varphi$ .

regenerative REGA device operating with pulse duration 180fs at a repetition rate of 250kHz. The output beam, frequency-doubled by second harmonic generation, provided the excitation beam of UV wavelength  $\lambda_P = 397.5\text{nm}$  and power 300mW. The horizontally polarized UV beam was then adopted to pump a non-linear BBO crystal, which generated pairs of photons with polarization  $\vec{\pi}_H$  and  $\vec{\pi}_V$  over the modes  $k_1$  with same wavelength  $\lambda = 2\lambda_P$ . This source allows us to obtain a high value of the gain  $g$ , which depends on the pumping power:  $g \propto \sqrt{P_{UV}}$ . Compared to conventional pulsed sources used to pump SPDC process, which achieve  $g \simeq 0.1$ , the energy per pulse is enhanced by a factor  $\simeq 400$ , leading to an increase of the gain value in the range of 20 – 40 depending on the focal length of the UV beam. The pumping power could be tuned adopting a half-wave plate and a polarizing beam splitter ( $\text{PBS}_{UV}$ ). The output state of BBO crystal with wavelength  $\lambda$  was spatially separated by the fundamental UV beam through a dichroic mirror (DM), then spectrally filtered adopting an interferential filter (IF) with bandwidth equal to 3nm and then coupled to a single mode fiber in order to select spatially a single mode of emission. A  $\lambda/2$  waveplate and a BBO with thickness of 0.75mm provided the compensation of walk-off effects. At the output of the fiber, after compensation (C) of the polarization rotation induced by the fiber, a phase shifting  $\varphi$  was introduced adopting a Soleil-Babinet compensator (B). The output radiation was then analyzed through a polarizing beam splitter (PBS) and detected adopting single photon detectors SPCM-AQR14 ( $D_1^A, D_1^B, D_1^C, D_2$ ). To characterize the detection apparatus, a coherent state with wavelength  $\lambda$  and polarization  $\vec{\pi}_H$  was fed into the mode  $k_1$ . The count rates  $D_1^A$  and the coincidence rates  $[D_1^A, D_1^B]$  were measured versus the phase  $\varphi$ : Fig.3. High visibility patterns have been observed with a period equal to  $\lambda$ .

As a first experimental step we have characterized the

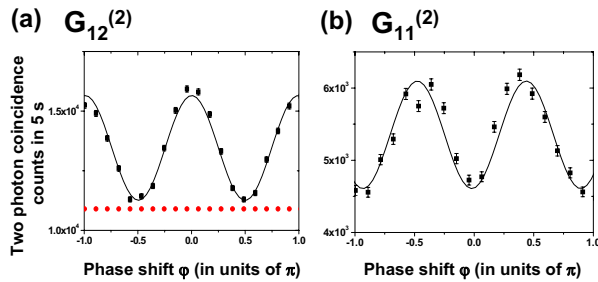


FIG. 4: (a)  $G_{12}^{(2)}$ : two-photon coincidence counts  $[D_1^A, D_2]$  versus the phase  $\varphi$  introduced by the Soleil-Babinet compensator ( $g = 1.4$ ). Circle data: expected accidental (without correlations) coincidence rates. (b)  $G_{11}^{(2)}$ : two-photon coincidence counts  $[D_1^A, D_1^B]$  versus the phase  $\varphi$  ( $g = 1.4$ ). Variations of the detectors signal ( $\sim 10\%$ ) due to different couplings of polarizations  $\vec{\pi}_H$  and  $\vec{\pi}_V$  with fiber have been corrected by normalizing coincidence counts with signal rates.

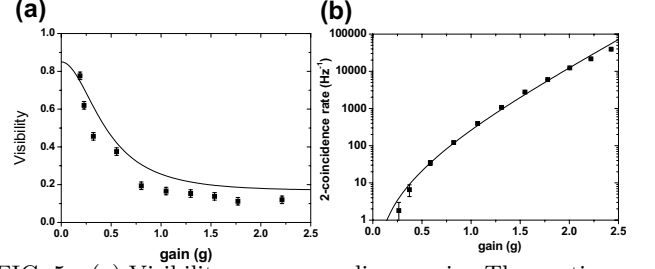


FIG. 5: (a) Visibility versus non-linear gain. The continuous line corresponds to the function  $V_{\max} \times V_1^{(2)}(g)$ . (b) Excitation rate versus non-linear gain. The continuous line corresponds to the function  $\bar{R}^{(2)}(\alpha g)$  where the parameter  $\alpha$  has been optimized by fitting the data and reads 0.85.

two-photon state generated by SPDC in the low gain regime. The visibilities have been found  $V_{12}^{(2)} = (85 \pm 2)\%$  and  $V_1^{(2)} = (80 \pm 1)\%$ . The discrepancy with the expected values  $V = 1$  is attributed to double-pair emission and to experimental imperfections. The same measurement has been carried out increasing the UV pump beam in order to measure the fringe patterns for different gain values. The gain has been estimated with the method introduced in Ref. [16, 17]. Fig. 4 refers to the configuration  $g = 1.4$ . The visibilities have been found to be  $V_{12}^{(2)} = (16.8 \pm 0.6)\%$  and  $V_1^{(2)} = (15 \pm 1)\%$ . The sub Rayleigh resolution is clearly shown by the experimental data of Fig.4. For the sake of completeness the value of  $V_1^{(2)}$  has been measured for different gains: Fig.5-a. The continuous line shows the expected theoretical function  $V_1^{(2)}(g)$  multiplied by the extrapolated visibilities for  $g \rightarrow 0 : V_{\max} = 0.85$ . We attribute the discrepancy between experimental and theoretical visibilities to partial multimode operation of the optical parametric amplifier [18].

To estimate the dependence of the excitation rate from the NL gain  $g$ , the maxima and the minima of the fringes have been measured versus the pumping power. The average data are reported in Fig.5-b. Our experiment validates the result found by Agarwal et al. [15] showing an exponential dependence on the parameter  $g$ . The expected two-photon excitation rate reads  $\bar{R}^{(2)} = 2\sigma^{(2)}(\bar{n} + 5\bar{n}^2)$  where  $\sigma^{(2)}$  is a generalized two-photon excitation cross section [15]. Fig.5-b shows how the excitation efficiency scales quadratically with the light intensity, in contrast with the two-photon SPDC regime; which leads to a linear dependence [19, 20, 21].

As further demonstration of the potentialities of the present approach, the simultaneous detection of three photons over the same mode has been investigated. The average three photon excitation rate reads  $\bar{R}^{(3)} = 12\sigma^{(3)}(7\bar{n}^3 + 3\bar{n}^2)$  where  $\sigma^{(3)}$  is a generalized three-photon excitation cross section and the visibility of the fringes is theoretically found as  $V_1^{(3)} = \frac{3\bar{n}+3}{7\bar{n}+3}$  [15]. Again a non-

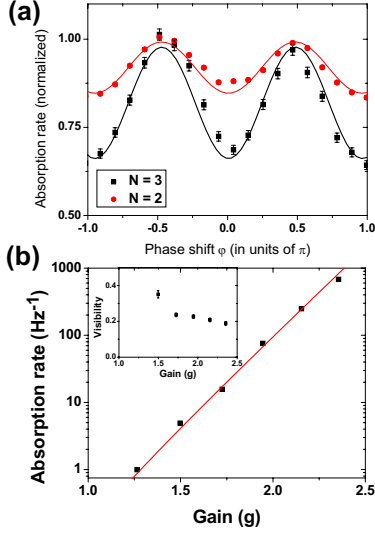


FIG. 6: (a) Circle data:  $G_1^{(2)}$  (two-photon coincidences  $[D_1^A, D_1^B]$ ) versus the phase  $\varphi$ ; Square data:  $G_1^{(3)}$  (three-photon coincidences  $[D_1^A, D_1^B, D_1^C]$ ) versus the phase  $\varphi$  ( $g = 2.4$ ) (b) Excitation rate versus non-linear gain. The continuous line corresponds to the function  $\overline{R}^{(3)}(g)$ . Inset: visibility  $V_1^{(3)}$  versus non-linear gain.

vanishing value of  $V_1^{(3)}$  is found for any value of  $g$ :  $V_1^{(3)}(g \rightarrow \infty) = \frac{3}{7}$  and the patterns exhibit a period equal to  $\frac{\lambda}{2}$ . Furthermore an increase of visibility is expected  $V_1^{(3)} > V_1^{(2)}$ . To demonstrate such a feature the three-photon coincidence rate  $G_1^{(3)}$  has been measured versus the phase  $\varphi$ : Fig.6-a. An increase of the visibility has been found  $V_1^{(3)} = (21.6 \pm 0.6)\%$ , the experimental dependencies of the three photon absorption rates and visibilities are shown in Fig.6-b.

In order to investigate the connection between the quantum feature of the state and the visibility of the fringe pattern, we have introduced a decoherence between the two polarization components  $\{\vec{\pi}_H, \vec{\pi}_V\}$  or  $\{\vec{\pi}_+, \vec{\pi}_-\}$  with a quartz crystal (Q) with a length equal to 20mm. This device introduces a temporal delay higher than the coherence time of the multiphoton fields. The  $G_1^{(2)}$  has been first measured without the quartz: Fig.7. When the decoherence affects the  $\{\vec{\pi}_H, \vec{\pi}_V\}$  components, we observe a reduction of visibility down to  $(4.8 \pm 0.6)\%$ ; on the other hand when the decoherence involves the  $\{\vec{\pi}_+, \vec{\pi}_-\}$  we observe the disappearance of the fringe patterns. The inversion of the maxima and minima of the square data compared to the circle data, a phenomenon not expected in the single-pair regime, is due to the reduction of the bunching effect among photons detected on the same polarization mode when decoherence is introduced.

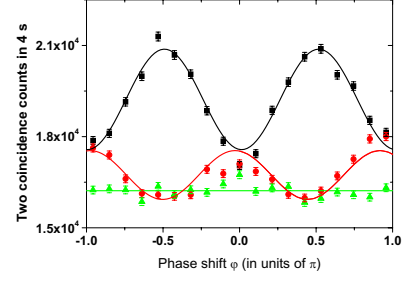


FIG. 7: Effects of coherence on fringe visibility. Square data: 2-photon coincidences counts versus the phase  $\varphi$  without introducing decoherence. Circle data: decoherence introduced between the polarization components  $\{\vec{\pi}_H, \vec{\pi}_V\}$ . Triangle data: decoherence introduced between  $\{\vec{\pi}_+, \vec{\pi}_-\}$ .

## CONCLUSIONS AND PERSPECTIVES

In the present paper we have experimentally demonstrated that the output state of a high-gain optical parametric amplifier can be intense; yet exhibits quantum features. We have extended the previous implementations [6], limited to the a-posteriori generation of a two photon state to a large number of photons. The reduced visibility has been increased by means of three-photon absorption as suggested by [15]. In this situation a higher visibility has been achieved but without an increase of the fringe density. The present article opens interesting perspectives for the implementation of a quantum interferometric setup. By adopting homodyne detection on the output fields, the Heisenberg limit for the phase resolution can be achieved [22]. Recently it has been proposed to combine high-gain SPDC with coherent states to create general NOON states with a fidelity of about 94% [23]. This work was supported by the PRIN 2005 of MIUR and Progetto Innesco 2006 (CNISM), ARO; DTO and DARPA.

- 
- [1] F. De Martini, et al., Progress in Quantum Electronics **29**, 165 (2005).
  - [2] A.N. Boto, et, Phys. Rev. Lett. **85**, 2733 (2000); P. Kok, et al., Phys. Rev. A **63**, 063407 (2001).
  - [3] M.J. Holland, Phys. Rev. Lett. **71**, 1355 (1993); J.P. Dowling, Phys. Rev. A **57**, 4736 (1998).
  - [4] J. Jacobson, et al., Phys. Rev. Lett. **74**, 4835 (1995); M. D'Angelo, et al., Phys. Rev. Lett. **87**, 0132602 (2001).
  - [5] K.T. Kapale, et al., quant-ph/0612196; H. Cable, et al., quant-ph/0704-067; A.E.B. Nielsen, et al., quant-ph/0704.0397.
  - [6] E.J.S. Fonseca, et al., Phys. Rev. Lett. **82**, 2868 (1999); K. Edamatsu, et al., Phys. Rev. Lett. **89**, 213601 (2002).
  - [7] M.W. Mitchell, et al., Nature (London) **429**, 161 (2004).
  - [8] P. Walther, et al., Nature (London) **429**, 158 (2004); T. Nagata, et al., Science **316**, 726 (2007).
  - [9] H.S. Eisenberg, et al., Phys. Rev. Lett. **94**, 090502

- (2005).
- [10] S.J. Bentley, and E.W. Boyd, Opt. Express **12**, 5735 (2004); A. Muthukrishnan, et al., Phys. Rev. Lett. **96**, 163603 (2006).
  - [11] D.V. Korobkin, et al., Opt. Eng. **41**, 1729 (2002).
  - [12] H.J. Chang, et al., Journal of Modern Optics **53**, 2271 (2006).
  - [13] G.S. Agarwal, et al., Phys. Rev. Lett. **86**, 1389 (2001).
  - [14] E.M. Nagasako, et al., Phys. Rev. A **64**, 043802 (2001); E.M. Nagasako, et al., J. Mod. Opt. **49**, 529 (2002).
  - [15] G.S. Agarwal, et al., J. Opt. Soc. Am. B **24**, 270 (2007).
  - [16] H.S. Eisenberg, *et al.*, Phys. Rev. Lett. **93**, 019301 (2004).
  - [17] M. Caminati, *et al.*, Phys. Rev. A **73**, 032312 (2006).
  - [18] S. Thanvanthri, et al., Phys. Rev. A **70**, 063811 (2004).
  - [19] J. Javanainen, et al., Phys. Rev. A **41**, 5088 (1990).
  - [20] J. Perina, et al., Phys. Rev. A **57**, 3972 (1998).
  - [21] B. Dayan, et al., Phys. Rev. Lett. **94**, 043602 (2005).
  - [22] O. Steuernagel, et al., J. Opt. B: Quantum Semiclas. Opt **6**, S606 (2004).
  - [23] H.F. Holfman, et al., quant-ph/0705.0047.